Article

Convectively Driven Polymerase Chain Reaction Thermal Cycler

E. K. Wheeler, W. Benett, P. Stratton, J. Richards, A. Chen, A. Christian, K. D. Ness, J. Ortega, L. G. Li, T. H. Weisgraber, K. Goodson, and F. Milanovich

Anal. Chem., **2004**, 76 (14), 4011-4016 • DOI: 10.1021/ac034941g

Anal. Chem. **2004,** *76,* 4011−4016

Convectively Driven Polymerase Chain Reaction Thermal Cycler

E. K. Wheeler,*,† W. Benett,† P. Stratton,† J. Richards,† A. Chen,† A. Christian,† K. D. Ness,†,‡ J. Ortega,† L. G. Li,† T. H. Weisgraber,† K. Goodson,‡ and F. Milanovich†

Lawrence Livermore National Laboratory, P.O. Box 808, Livermore, California 94551-0808, and Thermal Sciences Division, Stanford University, Stanford, California 94305

We have fabricated a low-cost disposable polymerase chain reaction thermal chamber that uses buoyancy forces to move the sample solution between the different temperatures necessary for amplification. Three-dimensional, unsteady finite element modeling and a simpler 1-D steady-state model are used together with digital particle image velocimetry data to characterize the flow within the device. Biological samples have been amplified using this novel thermal chamber. Time for amplification is less than 30 min. More importantly, an analysis of the energy consumption shows significant improvements over current technology.

Polymerase chain reaction (PCR) technology has facilitated DNA research in laboratories throughout the world.[1,2] PCR amplifies a target fragment of DNA, enabling identification. Successful PCR requires a sample to be thermally cycled between temperatures specific to the target DNA to be amplified. The three cycling steps in PCR are denaturation, annealing of primers to the template, and extension of the primers. The size and complexity of PCR devices have traditionally required that the DNA come to the laboratory. However, with the increase in use of these assays in research and clinical settings, PCR devices have undergone dramatic changes: from a large benchtop apparatus to a 2-lb battery-operated handheld device.[3]

If one has prior knowledge of the sequence of a biological agent, a PCR assay highly specific to that agent can be developed. Coupling this with portable instrumentation has put PCR into the hands of first responders (medical, military, or intelligence personnel) to a biological attack. Lawrence Livermore National Laboratory (LLNL) researchers have built several generations of biowarfare agent detection systems.[3−5] The jump from large benchtop machines to portable field-deployable devices was achieved with the advent of the microfabricated thermal chamber.[3−5] Fabricated from silicon and utilizing a disposable insert, the chamber enables PCR amplification in less than 7 min.[3,6] The smallest manifestation of portable PCR devices that utilize the silicon chamber is the Handheld Advanced Nucleic Acid Analyzer (HANAA). HANAA is currently licensed and manufactured for first responders to the scene of a biological attack or major catastrophe.[7] While other research groups have demonstrated small-scale PCR amplification,[8−10] the focus of this work is to demonstrate a low power consumption inexpensive thermal cycler that is disposable.

Building on LLNL's expertise in designing portable PCR units, we have developed a less expensive, more energy efficient disposable PCR thermal chamber that uses thermal convection to drive the PCR solution between the temperatures necessary for amplification.[11,12] This approach eliminates the need for an external driving mechanism and instead takes advantage of the temperature gradient present in the system. The driving force for the fluid motion is derived from the temperature-induced density differences while in the presence of a body force and is called the buoyancy force. Convectively driven flow is derived from the concept of natural convective-induced flow. Operating in a vertical plane, the difference between the denaturation and annealing/extension temperatures is sufficient to circulate the PCR solution in a closed loop. This work differs from previous flow-through devices in that no external pumping mechanism is necessary to move the fluid between the temperature zones since we have a closed loop.[11] Whereas, standard thermal cyclers actively heat and cool both the chamber and static fluid, the convectively driven polymerase chain reaction (CPCR) device predominantly heats only the fluid, thus increasing the thermal efficiency and, ultimately, reducing power consumption.

* Corresponding author: (e-mail) wheeler16@llnl.gov; (fax) (925) 422−2373.
† Lawrence Livermore National Laboratory.
‡ Stanford University.

(1) Mullis, K. B.; Faloona, F. *Methods Enzymol.* **1987**, *155*, 335.
(2) Sambrook, J.; Russell, D. W. *Molecular Cloning*, 3rd ed.; Cold Spring Harbor Laboratory Press: New York, 2001; Chapter 8.
(3) Belgrader, P.; Benett, W.; Hadley, D.; Richards, J.; Stratton, P.; Mariella, R., Jr.; Milanovich, F. *Science* **2000**, *284*, 449.
(4) Belgrader, P.; Smith, J. K.; Wedn, V. W.; Northrup, M. A. *J. Forensic Sci.* **1998**, *43*, 315−319.
(5) Northrup, M. A.; Benett, B.; Hadley, D.; Landre, P.; Lehew, S.; Richards, J.; Stratton, P. *Anal. Chem.* **1998**, *70*, 918−922.
(6) Northrup, M. A.; Mariella, R. P., Jr.; Carrano, A. V.; Balch, J. W. Silicon-Based Sleeve Devices for Chemical Reactions. U.S. Patent 5,589,136, December 31, 1996.
(7) Technology has been licensed to ETG who is developing the Bioseeq Handheld PCR Detector.
(8) Cheng, J.; Shoffner, M. A.; Hvichia, G. E.; Kricka, L. J.; Wilding, P. *Nucleic Acids Res.* **1996**, *24*, 380−385.
(9) Woolley, A. T.; Hadley, D.; Landre, P.; deMello, A. J.; Mathies, R. A.; Northrup, M. A. *Anal. Chem.* **1996**, *68*, 4081−4086.
(10) Lagally, E. T.; Medintz, I.; Mathies, R. A. *Anal. Chem.* **2001**, *73*, 565−570.
(11) Bennet, W. J.; Richards, J. B.; Milanovich, F. P. Convectively Driven PCR Thermal-Cycling. US Patent 6,586,233 B2, July 1, 2003.
(12) Wheeler, E. K.; Benett, W.; Ness, K.; Stratton, P.; Richards, J.; Weisgraber, T.; Papavasiliou, A. Laboratory Directed Research and Development FY2001 Annual Report, UCRL-LR-113717-01, 3−8, 2001. http://www-eng.llnl.gov/eng_llnl/01_html/pdfs/ETR_01_PDFs/ Vol1_LDRD.pdf.

10.1021/ac034941g CCC: $27.50
Published on Web 06/16/2004

Although convective forces are a new approach to thermal cycling for PCR, preliminary data indicated that they could, in fact, drive PCR amplification. In a simple test using HANAA, a polypropylene insert containing PCR reagents was partially withdrawn (to a height that allowed the fluid to cool to the lower temperature necessary for PCR) from the silicon heater set at the higher temperature. The Taqman optical detection scheme demonstrated PCR amplification. This result led to the design of an independent convective thermal chamber to fully investigate convective cycling as a new, robust approach to PCR.[11,12,13]

Krishnan et al. recently reported PCR amplification in a Rayleigh-Benard convection cell.[14] Their device consisted of a cylindrical cavity in a Plexiglas cube. [As will be discussed, geometry is a key parameter in establishing the necessary flow for a fluid element to traverse the required thermal environment and amplify.] Amplification of DNA required 1.5 h. Temperatures were controlled using a hot plate for the denaturation temperature and a water-cooled plate for the polymerization temperature. While the physics driving fluid flow between the necessary temperatures are similar to those used by Krishnan et al., our CPCR chamber design regulates the flow rate to achieve a more efficient PCR reaction. The geometry of our device (heating on the sides, instead of bottom) is sufficiently different from Krishnan et al. that Rayleigh-Benard convection is not the driving force in our device.

In this work, we report on the fabrication, characterization, and testing of a convectively driven PCR thermal chamber. The techniques used for fabricating the thermal chamber represent a departure from the former systems of silicon chambers. Three-dimensional modeling of the device explored the effects of geometric parameters before fabrication and will be presented briefly in this paper. Example systems, for proof of principle, include a 90-base pair (bp) multiple cloning site amplicon of plasmid DNA and both 58- and 160-bp amplicons of genomic *Erwinia herbicola* (Eh). Eh was studied because it is a nonpathogenic surrogate for plague (*Yersinia pestis*) a potential biowarfare agent as well as a naturally occurring disease. Finally, since one of the requirements for this thermal chamber is that the power consumption be low enough to run off a small battery, a brief power analysis is discussed.

MATERIALS AND METHODS

Convective PCR Thermal Chamber Design. The CPCR thermal chamber has fixed, constant temperature regions through which the sample flows, driven by buoyancy forces (Figure 1). Multiple heater zones (depicted as red and blue in Figure 1a) maintain the constant temperature zones of 94 and 55 °C. The sample is placed in a plastic bag made from thin polymer sheets. The bag is then sandwiched between two epoxy boards (containing resistive heaters and a layer of copper to ensure uniform heat transfer) forming the defined flow channel (Figure 1b). As the fluid in the hot section heats to 94 °C, thermal convection forces it to the cooler section, producing the required thermal cycling. We have demonstrated cycle times of 24 s. The multiple heating and cooling zones were integrated into the device to allow us the maximum flexibility in establishing the sample-dependent thermal profiles. Future devices will be fabricated with fewer temperature zones.

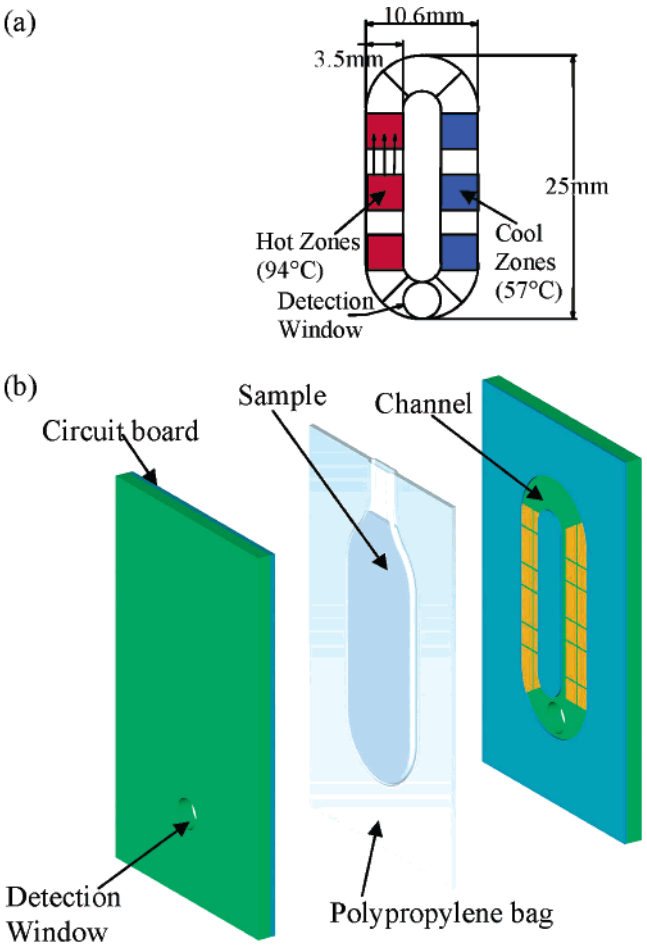

Figure 1. (a) Schematic of convective PCR thermal cycler and (b) rendering of convective PCR thermal chamber assembly. Sample is contained in the polypropylene bag sandwiched between the two circuit boards.

Thermal optimization is a key aspect of this design. PCR is highly temperature dependent so a stable temperature profile and good thermal control are critical aspects of the device. To limit power consumption, thermal capacitances are minimized. Conductive and convective losses on the hot side of the channel are balanced with the need for fast, yet passive, cooling on the cold side.

Fabrication of CPCR thermal cycler. The CPCR thermal cycler consists of two separate circuit boards assembled into one package. Layers of photolithographically patterned polymer films form the elliptic channel on each circuit board to create the fluidic structure. For the results presented here, each half of the channel was 200 μm deep, giving a total channel depth of 400 μm. However, channels varying in depth up to 1 mm can be formed. A specially designed 12-μm-thick polypropylene bag is loaded with the sample and sandwiched between the two thermal cycler circuit boards, forcing the sample fluid to conform to the channels in the circuit board (Figure 1b).

Off-the-shelf, surface-mount resistors and resistance temperature detectors are used as heaters and temperature sensors. Employing standard photolithography and etching techniques,

(13) Preliminary experiment performed in HANAA by W. Benett and J. Richards, May 27, 1999.
(14) Krishnan, M.; Victor M. Ugaz, V. M.; Burns, M. A. *Science* **2002**, *298*, 793.

copper on the back of the circuit board is patterned into power and sensing contacts for the surface-mounted elements. The mounting pads for the sensing and heating elements are directly opposite copper pads positioned in the channels on the fluidic face of the circuit board. The surface-mount devices are soldered to the mounting pads using standard electronics assembly techniques. An array of closely packed holes connects the device pads with pads on the channel side of the boards. These holes are filled with copper by electroplating to provide a low thermal resistance path for heat flow into the fluid.

PCR Amplification. For all PCR amplifications presented here the thermal chamber volume was 75 μL.

The PCR reagent mix consisted of 1-μL template, 0.15 mM forward primer, 0.15 mM reverse primer, 0.2 mM each dNTP (Roche Applied Science), 1.5 mM $MgCl_2$, 20 mM Tris-HCl pH 8.4, 50 mM KCl, and 5 units of platinum Taq polymerase (Invitrogen). Primers for the multiple cloning site segment of DNA were SP6 (TATTTAGGTGACACTATAG) and T7 (TAATACGACTCACTATAGGG) from Promega. Amplification of genomic Eh used primers Eh492F (GCTGCAAAACGCACAACA) and Eh550R (CGTGAACAAACGGCTCCA) from The Midland Certified Reagent Co.

The 90-bp multiple cloning site template used for CPCR amplification was obtained from an initial PCR using Promega's pGEM-13Zf(+) vector as the template. The 50-μL PCR mixture included 0.2 μg of template, 0.05 μM SP6 primer, 0.05 μM T7 primer, 1 mM each dNTP (Roche Applied Science), 2.5 mM $MgCl_2$,10 mM Tris-HCl pH 8.3, 50 mM KCl, with 5 units of AmpliTaq Gold polymerase (Applied Biosystems). A PCR thermal program of an intial 95 °C for 5 min, 30 cycles of 95 °C for 60 s followed by 56 °C for 60 s, with a final soak at 72 °C for 3 min was performed in an MJ Research PTC-200 thermocycler. This initial PCR's 90-bp product was then diluted 1:100 in double-distilled H_2O for use as a template in the CPCR device. Amplification was confirmed by running electrophoretic gels (4% NuSieve 3:1 Plus agarose gels manufactured by Latitude). Gels were typically run at 80 V for 30 min.

Digital Particle Image Velocimetry (DPIV). DPIV is a noninvasive, optical technique for measuring fluid velocity fields with high spatial resolution.[15,16] The spatial resolution is dictated by the imaging optics, particle size, and processing parameters, whereas temporal resolution is governed by the light source and recording electronics. For our device, the flow was seeded with 2-μm fluorescent polystyrene beads (Molecular Probes) and imaged through the 3-mm detection window using a mercury lamp and a 5× objective. A Pulnix 1040 CCD camera acquired images at a 1000 by 1000 pixel resolution. Since the CPCR device had to be oriented vertically, the Zeiss microscope was reconfigured to create a horizontal optical path. Data from 250 images were analyzed to produce the average velocity profile in the channel with spatial and temporal measurement resolutions of 60 μm and 15 Hz, respectively.

RESULTS AND DISCUSSION

Modeling. Since the convective PCR thermal cycler was in its nascent stage and had never been used to drive PCR flows before, two models were developed to understand the important device parameters before the first prototype was submitted for fabrication. The models varied in rigor and complexity, but both accounted for buoyancy-driven flow and heat transfer in the device. A detailed 3-D finite element calculation was performed using the supercomputers available at LLNL. In parallel, an approximate 1-D model that captures the heat and mass transfer was developed using internal flow, analytical results, and a force balance, yielding rapid predictions that agree well with both the 3-D finite element modeling and the experiments.

3-D Fluid Dynamic Modeling. 3-D modeling of the system was performed using a finite element incompressible flow code. The geometry and dimensions of the device were entered into a nonuniform grid that allowed better resolution of the flow behavior near the walls. The boundary conditions were no slip/no penetration with adiabatic temperature boundary conditions. The fluid properties were assumed to be those of water and were considered independent of temperature (Boussinesq approximation). While we acknowledge that some of these properties do change with temperature, the model at this time does not take this into account. Initially, the fluid velocity is zero. At time zero, the temperature boundary conditions are turned on. The computations were performed using both implicit and explicit, first-order accurate time integration schemes for an 18 432-element grid.[17] Using the explicit method simulations required 13 days on super computers. There is less than 3% error between the implicit and explicit methods. Once the system reached steady state, the velocity magnitude changed less than 0.005%.

The vertical velocity component at the midplane along line A−A across the straight region of the loop is shown in Figure 2a. The maximum fluid velocity is 2.3 mm/s. A profile of the horizontal component of the velocity around the curve (along line B−B) is plotted in Figure 2b, with a maximum velocity of 2.9 mm/s. Clearly, fluid elements at the inner surface have shorter cycle times than those nearer the outside. This distribution in cycle times will result in a distribution of amplification times. However, diffusion of DNA fragments across streamlines helps smooth out this distribution. Across the 400-μm depth of the channel, the simulations show parabolic velocity profile.

Steady State 1-D Model. The 1-D model reduces the loop to steady-state conditions in a periodic channel, reducing the computation time from days or hours on a supercomputer to 5 min on a desktop personal computer. The net force driving fluid flow is proportional to the mass difference of the respective columns of fluid on the hot and cold sides of the loop ($force_{hot} < force_{cold}$), which are governed by their temperature differences and local densities. The difference in mass, therefore, yields a pressure gradient along the channel and a flow rate can be approximated using classical results for laminar internal flow. Additional pressure differences at corners are neglected. In the heater regions of the channel, temperature boundary conditions were applied with the heat-transfer rate to the fluid governed by the Nusselt number for internal flow.[18] In the unheated connecting regions of the cycle, heat is lost to the environment through an

(15) Adrian, R. J. *Int. J. Heat Fluid Flow* **1986**, *7*, 127−145.

(16) Willert, C. E.; Gharib, M. *Exp. Fluids* **1991**, *10*, 181−193.

(17) Ness, K. D., manuscript in preparation.

(18) Shah, R. K., London, A. L. *Laminar Flow Forced Convection in Ducts*; Academic Press: New York, 1978; pp 213-218.

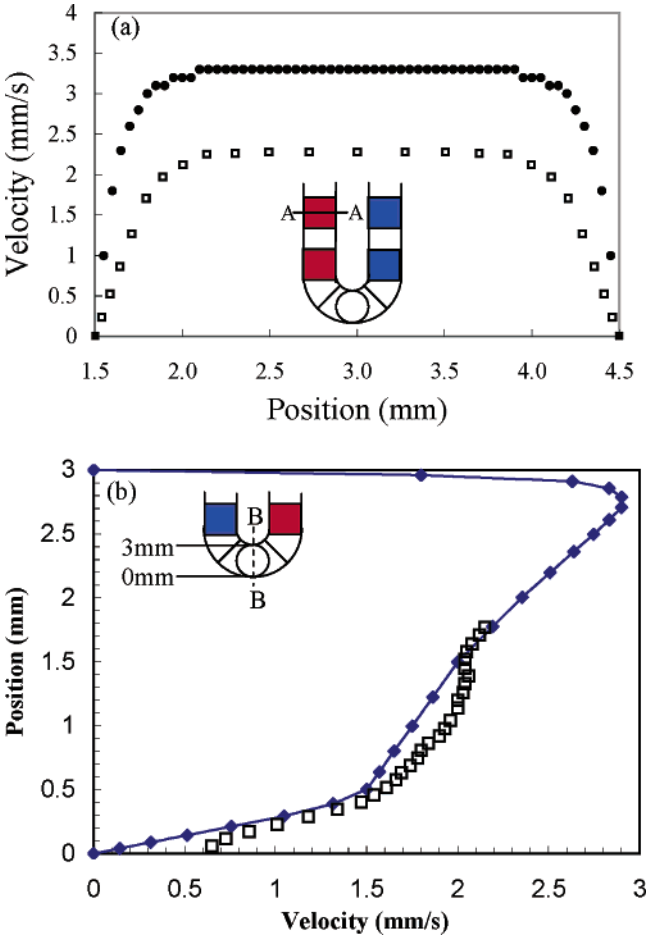

Figure 2. Directional components of the velocity along lines shown in figures. (a) Vertical velocity across the straight section of the channel. 3-D model represented by open squares and solid circles are 1-D model predictions. (b) Horizontal velocity along B−B from 3-D model (solid diamonds) and experimental measurements of velocity from DPIV (open squares).

inclusive thermal resistance parameter. A detailed discussion of this model will be presented in a future publication.[17]

The 1-D model predicts a maximum velocity of 3.3 mm/s. Since the 1-D model neglects flow around corners by straightening the channel into a straight rectangular channel, it is not surprising that the 1-D model predicts a slightly inaccurate velocity. When corner effects are included in the 1-D model this will reduce the average velocity due to a larger fluidic resistance through the region bringing the models in closer agreement. Unfortunately, due to the location of the window, fluid visualization could not be performed on the straight part of the channel for a direct comparison with the 1- and 3-D models. However, the simplified 1-D model is in good agreement with the complete 3-D simulation (Figure 2a), indicating that the 1-D model is a valuable design tool.

Modeling allowed us to investigate the effects of certain geometrical parameters before fabrication. For example, simulations allowed us to minimize the length of heaters. 3-D simulations proved that we could generate enough buoyancy force with a heater half of the original proposed length. With the goal of minimizing energy consumption, the models allowed us to move from a single continuous heater to three smaller heaters. The

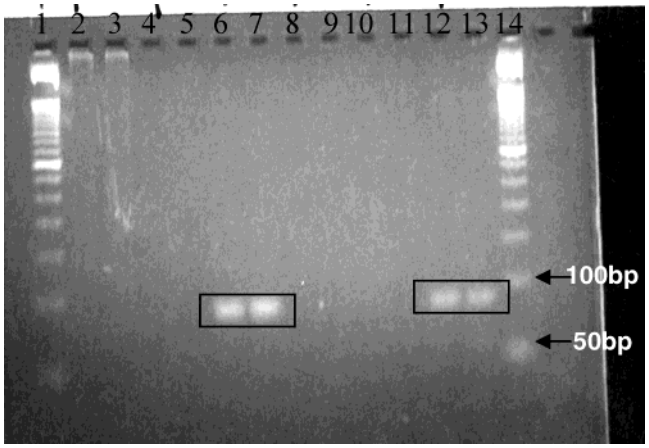

Figure 3. Amplification of 90-bp multiple cloning site DNA segment. Black arrows point to the bands from the 50- and 100-bp DNA markers. As controls, samples in lanes 2−7 were amplified in an MJ Research thermal block. Lanes 8−13 were amplified in the CPCR device. The contents of each lane are as follows: (1) 50-bp ladder, (2, 3) negative control of master mix with no DNA, (4, 5) negative control with no enzyme, (6, 7) positive control of 90-bp MCS DNA, (8, 9) negative controls without template DNA, (10, 11) negative controls without enzyme, (12, 13) CPCR, and (14) 50-bp ladder.

models also allowed us to predetermine the optimum channel depth for the desired amplification time.

Convective Flow Characterization. The details of the flow inside the thermal chamber were investigated using DPIV. The velocity profile across the lower portion of the detection window is included in Figure 2b (open squares). There is excellent agreement between the experimentally measured velocity profile and the simulation. Due to the compliant nature of the bag, surface irregularities complicated the imaging process in the upper region of the detection window and prevented an accurate measurement of the velocity profile at that location. This issue is being resolved for a complete comparison across the entire channel width. As expected, DPIV shows a range of velocities (0.6−2.2 mm/s) across the detection window with an average fluid velocity of 2 mm/s. Since this is an average measurement, the error is less than 1%. Therefore, a particle following a streamline in the center of the channel will experience 30 cycles in ∼12 min.

Amplification in CPCR Thermal Cycler. Amplification using the CPCR thermal cycler was first demonstrated on the 90-bp segment from a multiple cloning site segment of DNA. Starting concentrations ranged from 10^5 to 10^7 copies/mL. Figure 3 shows an agarose gel of the sample after amplification in the CPCR thermal cycler (see lanes 8−13). Amplification in the CPCR thermal chamber is compared to amplification in a standard benchtop MJ Research block thermal cycler instrument. Negative controls for both devices consisted of just the master mix with no template DNA or no enzyme.

Figure 3 clearly shows we successfully amplified the 90-bp segment of DNA in the convective PCR thermal chamber. The 90-bp bands both from the traditional cycler and the CPCR cycler have been highlighted with boxes for easy comparison. As expected, no bands are present in the negative control lanes. For this particular run, the CPCR device ran at steady state for 30 min. It should be noted that the device is not yet optimized to minimize the amplification time. Studies of the MCS DNA were simply intended as proof of principle. It should be noted that the

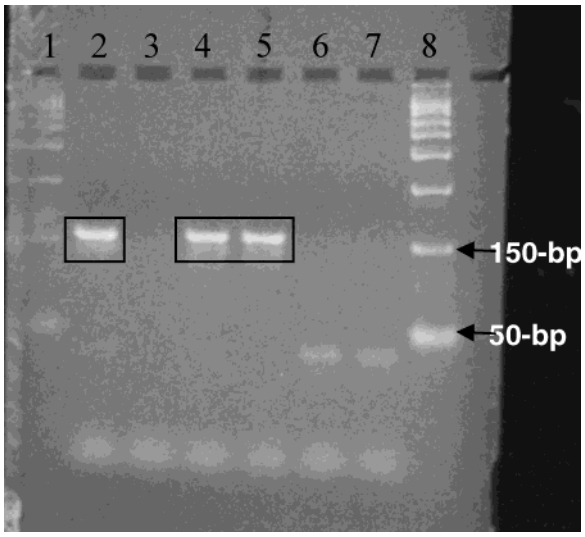

Figure 4. Amplification of 160-bp segment of Eh. Starting concentration is 10^5/mL. Lanes 1 and 8 contain DNA markers (50, 150, 300, ... bp). Black arrows point to the bands from the 50- and 150-bp DNA markers. Wells 2 and 3 are positive and negative controls, respectively, performed on an MJ Research thermal cycler. Wells 4 and 5 are two aliquots from a CPCR run. Likewise, wells 6 and 7 are negative controls from a CPCR run.

bands from the CPCR device appear fainter than those from the MJ Research thermal cycler. One reason for this is the different thermal profiles that the two cyclers generate. For example, in one cycle on the MJ Research thermal cycler, a sample experiences both 95 and 56 °C for 60 s each. By comparison, in the convectively driven PCR thermal cycler, a sample sees both of these temperatures in ~24 s. Differences in the thermal profile will affect the amplification efficiency.

Amplification of a biologically relevant segment is presented next. As stated earlier, Eh was chosen for its relevance to both medical and biowarfare arenas. Both 58- and 160-bp segments of Eh were amplified in the CPCR device. A gel of an amplification of the 160-bp amplicon is shown in Figure 4, demonstrating that we successfully amplified an Eh segment using our convectively driven thermal cycler.

Experimental studies to minimize the amplification time indicate that it can be shortened from 30 to 20 min (after a 9-min start-up time). However, further reducing the amplification time to 10 min does not yield amplification. For the experiments presented in this paper, we have been using a slow temperature ramp to reach steady state to avoid overheating. We are currently performing experiments to decrease the start-up time, to further minimize the energy consumption of the CPCR thermal cycler.

Power Analysis. Analysis of the current state-of-the-art HANAA, designed at LLNL, shows that only a relatively small percentage of the energy imparted to the thermal chamber is needed for cycling the fluid between the two temperatures with the majority of the energy escaping to the environment. Therefore, redesigning the thermal chamber will decrease the power consumption of the PCR unit significantly. This lower power requirement will potentially allow the thermal chamber to run with a wristwatch battery. This will in turn significantly reduce the unit size and weight, and more importantly, the technology advancement will enable us to take major steps toward the next generation of portable, disposable PCR devices.

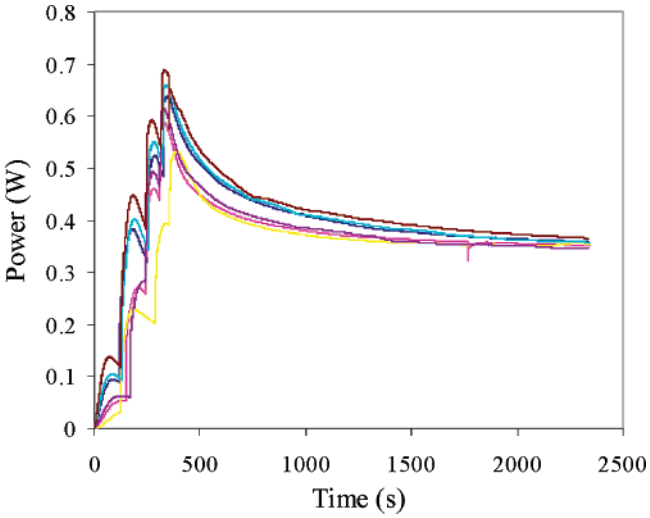

Figure 5. Power consumption of CPCR thermal cycler for five 39-min amplifications. Average total energy consumed for these runs is 866 ± 55 J.

Table 1. Comparison of Energy Consumption for CPCR Disposable Device and HANAA, the Current State-of-the-Art Portable PCR Device

	HANAA	CPCR
volume (μL) of fluid	25	75
energy for fluid[a] (J)	210	630
energy input to device/run (J)	3200	866
% energy to fluid	6.5	72

[a] Based on 50 cycles per run.

A typical plot of power consumption during an amplification run is shown in Figure 5. As stated earlier, these results came from runs that were not optimized for power reduction. Temperatures were slowly ramped to their equilibrium values over 9 min. Once equilibrium was reached, amplification proceeded for 30 min. We are continuing experiments to decrease startup times and amplification times. Integrating the area under the power curves yields the energy consumed by the thermal cycler. Five separate runs, all resulting in PCR amplification, consume an average energy of 866 ± 50 J (for just the thermal cycler). By comparison, an AA Ni metal hydride (1.2 V) battery has a capacity of 5184 J.

The central energy consumption requirement is to heat an aqueous fluid from room temperature to 95 °C and then to cycle the fluid between 55 and 95 °C. A maximum of 50 cycles will be used. Thus, the basic heat requirement (based only on cycling the fluid, with a heat capacity similar to water) is 8.4 J/(μL/run). For a75-μL sample size, this results in a basic energy requirement of 630 J/run. In addition to this basic requirement, there will be heat capacitances in the structural components and heat losses to the environment.

Compared to existing field-deployable technologies (HANAA), the CPCR thermal chamber shows a significant improvement in energy consumption. Table 1 summarizes the energy consumption for the two devices. Since the two devices differ in volume, it is best to compare the ratio of the amount of energy for an ideal system that uses all energy to heat the fluid (row 2) to the energy actually consumed by the device (row 3). The CPCR

device exhibits an order of magnitude improvement over the HANAA.[19]

CONCLUSIONS

We have successfully fabricated and demonstrated a convectively driven PCR thermal chamber. The device has also been manufactured from low-cost materials to be disposable. Not only are the polypropylene bags disposable but the entire thermal cycler is inexpensive enough that it can also be disposable. By using thermal convection to drive the fluid between the temperatures necessary for PCR amplification, we have dramatically decreased the energy consumption of the device. PCR validation has been performed on a biologically important surrogate, *E. herbicola*. We anticipate that this new and more efficient PCR device will see widespread use not only in the field but also in research and development and could ultimately become pervasive in diagnostics such as food quality control, medical diagnostics, and environmental monitoring, as well as a low-cost diagnostic for the third world.

(19) HANAA data supplied by Paul Stratton.

ACKNOWLEDGMENT

This project was funded by Engineering Exploratory Research and Development funds from the Laboratory Directed Research and Development program. Funding from this program is gratefully acknowledged. Linwood Manchester, Robert Augenthaler, and Mario Toporco in the circuit board shop and Daniel Schumann and Inge Fine in the plastic shop are thanked for their innovations to manufacture the device. We thank Lara Daily for preliminary 3-D modeling results. K.D.N. thanks David Clague for useful discussions about the 1-D steady state model. This work was performed under the auspices of the U.S. Department of Energy by University of California, Lawrence Livermore National Laboratory under Contract W-7405-Eng-48.

Received for review August 11, 2003. Accepted December 9, 2003.

AC034941G